



# Separation of Fe and Mn from Manganiferous Iron Ores via Reductive Acid Leaching Followed by Magnetic Separation

Soner Top<sup>1</sup>

Received: 25 March 2019 / Accepted: 16 July 2019 / Published online: 1 August 2019  
© Society for Mining, Metallurgy & Exploration Inc. 2019

## Abstract

In this study, a process to separate manganese and iron from manganiferous iron ores by reductive acid leaching followed by magnetic separation was conceived and experimentally tested. In the leaching process, sulfuric acid was used as lixiviant and oxalic acid was used as reductant. The experimental results showed that the manganese and iron separation was optimum when the concentration of the sulfuric acid and oxalic acid were 0.75 M and 30 g/L, respectively, at a temperature of 80 °C, a solid/liquid ratio of 67 g/L, stirring speed of 400 rpm, and leaching duration of 60 min. Under this condition, 90.49% and 6.78% of Mn and Fe were dissolved, respectively, from the ore sample with a size fraction of  $-106 \mu\text{m}$ . It was determined that the leaching of manganese from the ores was a second-order reaction with an activation energy ( $E_a$ ) of 53.38 kJ/mol. The leaching residues obtained under the optimum condition were subjected to high-intensity wet magnetic separation tests to recover the remaining iron content. This separation process produced a concentrate containing 56.20% Fe and 1.79% Mn with iron and manganese recoveries of 56.83% and 66.73%, respectively. A magnetic separation test from an unleached ore sample was also carried out as a benchmark. To the best of our knowledge, this is the first time that a magnetic separation process was used to a residue obtained from reductive acid leaching of manganiferous iron ores to recover iron.

**Keywords** Manganiferous iron ores · Leaching · Reductant · Magnetic · Separation

## 1 Introduction

Iron and manganese ores are indispensable raw materials for iron and steel industries. The vast majority of iron ores are used in steel production. Iron ores such as hematite, magnetite, and limonite are also used in cosmetics, paint, medicine, and chemical industries [1–3]. Similarly, more than 90% of manganese ores are utilized in the steelmaking process, while the rest is used to produce dry-cell batteries and various chemical reagents, glasses, ceramics, fertilizers, and animal feeds [4]. Manganese not only improves the strength of a steel but also plays an important role as deoxidizers and desulfurizers in steel production [5]. As a result of the increasing demand for iron and steel products, the production of manganese and iron

ores tends to increase with time. This is evident from the increase in mine production of manganese by 29% in the last decade, from 14 million tons in 2008 to 18 million tons in 2018 [6]. Similarly, though to a lesser extent, the production of iron ore was increased by 13% in the last decade, from 2.2 billion tons in 2008 to 2.5 billion tons in 2018 [7].

Manganese enters the structure of mafic minerals together with iron ions during the crystallization stage of magma. Therefore, most manganese deposits contain iron compounds. As a transition metal, manganese is very similar to iron in terms of geological formation conditions, chemical and physical properties [8]. In addition, these two elements are next to each other in the periodic table, which shows how chemical elements are related to each other.

There are three types of ores that contain a concentrated amount of manganese based on its iron content, namely manganese ores ( $>35\%$  Mn and without Fe), ferrous manganese ores ( $25\% < \text{Mn} < 35\%$  and  $13\% < \text{Fe} < 23\%$ ), and manganiferous iron ores ( $10\% < \text{Mn} < 25\%$  and  $\text{Fe} < 48\%$ ) [9]. In addition to hydrothermal, sedimentary, residual, and metamorphic deposits, polymetallic deep-sea manganese nodules are recently considered to be valuable natural resources of manganese [10, 11]. Not only manganese but also non-ferrous

**Electronic supplementary material** The online version of this article (<https://doi.org/10.1007/s42461-019-00113-8>) contains supplementary material, which is available to authorized users.

✉ Soner Top  
soner.top@agu.edu.tr

<sup>1</sup> Materials Science and Nanotechnology Engineering Department, Abdullah Gül University, 38080 Kayseri, Turkey

metals such as copper, nickel, and cobalt can be efficiently beneficiated from the nodules [12, 13].

Iron ores can easily be separated from the gangues by exploiting the differences in specific gravity, magnetic, and surface properties [14–16]. In addition, it is possible to obtain manganese with a high recovery from manganese ores containing a trace amount of iron via gravity separation methods [17, 18]. The presence of manganese in the iron ores, however, makes the separation process more complex due to its similar physical and chemical characteristics to iron [19–23]. Manganese can be extracted from its oxide ores by either reduction roasting–magnetic separation, reduction roasting–acid leaching, or direct reductive leaching [24–26]. Direct acid leaching in the presence of ZnS or used as oxidants for metal sulfides is an alternative leaching method to treat manganese ores [27, 28]. The carbothermal reduction processes using coal, CO, or CO<sub>2</sub> as a reductant can be used to treat complex manganese ores to convert MnO<sub>2</sub> and Fe<sub>2</sub>O<sub>3</sub> into non-magnetic MnO and ferromagnetic Fe<sub>3</sub>O<sub>4</sub>, respectively. Microwave reduction methods, which are different from the conventional roasting methods with main features including selective heating and low energy consumption, have been preferred recently [29]. Several studies have demonstrated that magnetic separation methods can be used to separate iron from manganese ores after reductive roasting [30–32]. However, a metallurgical process involving magnetic separation following a reductive leaching of the ores to separate iron from manganese has not been studied before.

High temperatures in the range of 500 to 1000 °C are required to reduce manganese ores by pyrometallurgical methods. This leads to high energy consumption. Following the high temperature reduction process, wet magnetic separators are often used [33]. This process sequence involves material migration from a dry to wet mediums, making the process difficult in terms of process continuity. The present study attempts to minimize this difficulty by using a hydrometallurgical process to reduce the manganese from the ores. Recently, selective reduction of manganese from the ores can be achieved with the use of oxalic acid [34], sawdust [35], cornstalk [36], molasses [37], carbohydrates [38, 39], corncob [40], guar meal [41], waste tea [42], CaS [43], or lignin [44] as reductant. Compared with a pyrometallurgy process, the use of a hydrometallurgical process also provides some advantages such as less pollution, lower energy consumption, and simpler equipment [45].

Sulfuric acid is the most widely used acid for leaching because of its availability, low cost, and selectivity against manganese. The selectivity against iron can be enhanced by increasing the temperature or by introducing alkali metal ion such as ammonium ion [46]. Organic acids are considered as both an easy and effective green leachates and take a leading role as reducing agents for the hydrometallurgical manganese production as they do not emit hazardous gas during leaching and require simple purification of the leach solution. They are

also efficient and easily accessible. The dissolution of manganese can be as high as 100% with low iron co-dissolution when oxalic acid is used as a reducing agent instead of the other reducing agents [47, 48].

Direct reduction leaching of Fe-Mn ores with oxalic acid provides better selectivity. In this route, reductants are added to reduce Mn<sup>4+</sup> into Mn<sup>2+</sup> during the acid leaching process [49]. Sahoo et al. (2001) dissolved 98.4% of Mn and 8.7% of Fe from –150 + 105 mm low-grade manganese ore using 0.543 M sulfuric acid as lixiviant and 30.6 g/L oxalic acid as oxidant at 85 °C at the end of 105 min with a solid-to-liquid ratio of 1:20 [35]. Azizi et al. (2002) extracted 93.44% of Mn and 15.72% of Fe from low-grade manganese ores using 7% of H<sub>2</sub>SO<sub>4</sub> as lixiviant and 42.50 g/L oxalic acid as reductant at 65 min and 63 °C [50]. Sayilgan et al. (2009) studied manganese and zinc recovery from the spent alkaline and zinc-carbon batteries. After the leaching tests, 91% of Mn and 112% of Zn were dissolved by using 30% of oxalic acid together with 30% of H<sub>2</sub>SO<sub>4</sub> at 45 °C after 3 h of leaching with %10 pulp density [51]. El Hazek and Gabr (2016) extracted 98.2% of Mn from a complex polymetallic ore using 0.24 M of oxalic acid as a reductant in 0.5 M H<sub>2</sub>SO<sub>4</sub> medium after 105 min of leaching at 85 °C [52]. Astuti et al. (2019) used different reducing agents such as glucose, molasses, tannic acid, oxalic acid, fructose, green tea, cane sugar, sodium sulfite, citric acid, black tea, cellulose, sawdust of candlenut shell, sawdust of Acacia wood, sawdust of coconut shell, sawdust of *Albizia chinensis* wood, and H<sub>2</sub>O<sub>2</sub> to extract Mn from a manganese ore. After the reductive acid leaching tests, they concluded that oxalic and tannic acid were found to be the most effective reducing agents for the H<sub>2</sub>SO<sub>4</sub> leaching process. The Mn recoveries were 100% under the conditions of 5% of pulp density with 1 M of H<sub>2</sub>SO<sub>4</sub> at 30 °C of leaching temperature, 150 rpm of stirring speed, and 8 h of leaching time with reductants/ore ratio of 0.75 g/1.5 g [53]. As an alternative to sulfuric acid, the other inorganic acids such as hydrochloric and nitric acid have also been used as lixiviant [54, 55]. Practically, sulfuric acid is the most preferred lixiviant given its economic advantages over the other lixiviants.

Although manganese oxides are used in iron and steel production due to their desulfurization and deoxidation capabilities, manganese grades in iron ores fed to furnaces should be < 1.5% Mn for direct charge ore and < 5% Mn for sintered ore [56]. This is because Mn has a negative effect on iron ore reduction. It causes heterogeneous reduction and increasing slag formation in which valuable iron ores could be found [57]. Likewise, the Mn/Fe ratio of manganese ores should be over 5 for ferromanganese manufacture [58].

This study aims to separate Mn and Fe from manganiferous iron ores using direct reduction leaching followed by magnetic separation. This has not been reported in the literature before. The study consists of two stages: (1) selective dissolution of Mn from the ore by a reductive acid leaching and (2) recovery of Fe from the leach residue using high-intensity wet magnetic

separation. In addition, the control tests were used to the non-leached samples to reveal the difference in magnetic separation.

## 2 Experimental

The ore sample used in this study was collected from the Ceyhan district of Adana province in Turkey. The mine has 76,557 tons of visible and probable manganese iron ores reserve [59]. The sample was crushed, ground, and screened to  $-106\ \mu\text{m}$ . Reductive sulfuric acid leaching was performed to the sample using oxalic acid as reductant. Tap water was used together with the analytical grade chemicals in leaching and magnetic separation experiments to simulate real industrial processing conditions. Mn and Fe values in tap water were measured and excluded from the leach solutions. The chemical contents were determined by AAS (PinAAcle 900 H) and XRF (Minipal 4) analyses. XRD devices (Bruker Discover D8 and Rigaku Miniflex) were used for the phase identifications. The flowchart of the study is shown in Fig. 1. The goal of this study was to obtain the manganese in a liquid form and the iron in a solid form.

Hybrid test designs invented by Roquemore (1976) [60], which is one of the response surface methodologies, have been used for the selection of effective leaching parameters. A hybrid design for  $n$  factors can be created using a central composite design (CCD) for  $n - 1$  factors. The design requires 5 levels for each factor. Significant Roquemore hybrid designs are the 311, the 416, and the 628. These designs are rotatable or near to rotatable. The first number in the name refers to the number of factors and the next two numbers indicate the number of experiments [61].

A hybrid design coded as the 311, consisting of 3 factors and 11 experiments, was used in this study. The Fe and Mn

### Manganiferous iron ores

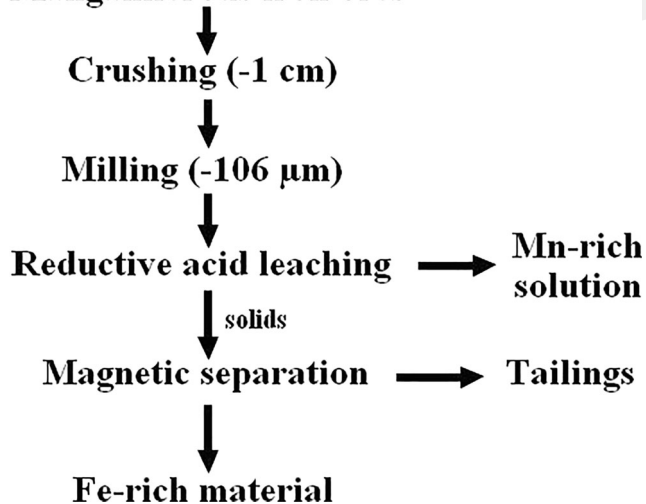


Fig. 1 Flowchart of the experimental procedure

extraction values (%) were recorded as responses. The results were evaluated and 3D graphs were created by the Design Expert 11 software. The high values were 1.00 M, 50 g/L, and 150 min, and the low values were 0.50 M, 10 g/L, and 30 min for  $\text{H}_2\text{SO}_4$  concentration,  $\text{C}_2\text{H}_2\text{O}_4$  concentration, and leaching time, respectively. In addition to the prior knowledge mentioned, the determination of lower and upper levels was influenced by the desire to develop an environmental, economic, and sustainable process using as little resource as possible. Hybrid design tests were conducted at room temperature. The best leaching condition of the hybrid design was determined and then the effects of leaching temperature on Fe and Mn extractions were investigated. Leaching tests were carried out by a temperature-controlled magnetic stirrer at atmospheric pressure. For each experiment, 20 g of sample was leached in a 500-mL beaker, which was covered with a watch glass to minimize evaporation losses, with 300 mL of sulfuric acid and oxalic acid at a predetermined concentration and temperature. The iron-rich residue obtained under the optimum leach condition was subjected to magnetic separation using a high-intensity wet magnetic separator (Eriez L4-20 WHIMS). The pulp, conditioned in a 250-mL vessel by mechanical stirrer during 3 min, was fed to the magnetic separator adjusted to specific magnetic field strength. The solid/liquid ratio was 300 g/L for magnetic separation tests. The stirring speeds were 400 rpm in all separation experiments. Samples dried at  $80\ ^\circ\text{C}$  until a constant weight were obtained. Magnetic separation experiments were performed before and after leaching experiments and the Mn and Fe recoveries and grades were compared. The recoveries for leaching and magnetic separation tests were calculated by Eq. 1 and Eq. 2, respectively.

$$Y = \frac{D}{T} \times 100 \quad (1)$$

$$Y = \frac{M \times m}{F \times f} \times 100 \quad (2)$$

where  $Y$  is the yields of Fe or Mn (%),  $M$  is the mass of magnetic product (g),  $m$  is the Fe or Mn grades of the magnetic product (%),  $F$  is the mass of feed sample (g), and  $f$  is the Fe or Mn grades of feeding (%).  $D$  is dissolved Fe or Mn (mg) and  $T$  is the total Fe or Mn in feeding (mg).

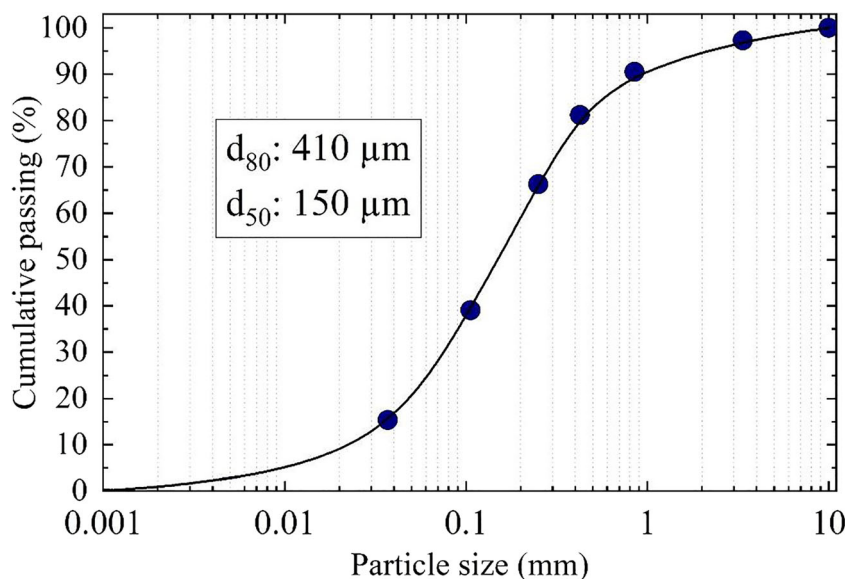
## 3 Results and Discussions

### 3.1 Sample Characterization

The particle size distribution of the ground samples was given in Fig. 2. All the particles analyzed were smaller than 5 mm and the  $d_{80}$  value was  $410\ \mu\text{m}$ .

The Fe and Mn grades for certain particle size ranges were determined by size-wise analysis (Table 1). It was observed

**Fig. 2** Cumulative undersize curve of the sample (logarithmic scale)



that Mn grades increased as the grain sizes increased. The concentration of Mn exceeded 15% at sizes bigger than 1.12 mm. The highest Fe concentration (40.76%) was obtained at a particle size fraction between 0.85 and 1.12 mm.

The degree of liberation is an important criterion for mineral separation. In addition, the determination of this size prevents excessive grinding and extra chemical consumption. In this way, economic benefits are achieved through a target-oriented approach. Microscope images of the materials were examined at certain particle sizes to determine the liberation size (Fig. 3).

It was observed that the red and black parts (Fe and Mn minerals) and the white and gray parts (quartz, calcite, and clay) began to be liberated at 300  $\mu\text{m}$  in size. A better liberation was achieved under 106  $\mu\text{m}$  in size. This size fraction (0–106  $\mu\text{m}$ ) is used in the separation tests because it did not only provide high liberation degree but also gave the lowest Fe and Mn grades. The chemical analysis of the sample was presented in Table 2.

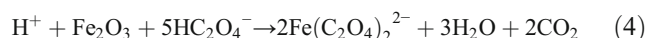
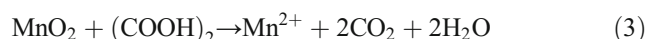
The XRD pattern of the sample is shown in Fig. 4. Approximately, 82% of the sample had a crystalline structure while the rest was amorphous. The crystalline portion contains

34.5% hematite ( $\text{Fe}_2\text{O}_3$ ), 13.8% manganite ( $\text{MnO}(\text{OH})$ ), 12.3% quartz ( $\text{SiO}_2$ ), 7.2% ferrian grossular ( $\text{Ca}_3\text{Al}_{1.6}\text{Fe}_{0.4}\text{Si}_3\text{O}_{12}$ ), 4.8% manganese (VII) oxide ( $\text{Mn}_2\text{O}_7$ ), 2.5% ramsdellite ( $\text{MnO}_2$ ), 8.1% wollastonite-manganite ( $(\text{CaMn})\text{Si}_2\text{O}_6$ ), 11.1% macfallite ( $\text{Ca}_2(\text{Mn}^{+3}, \text{Al})_3(\text{SiO}_4)(\text{Si}_2\text{O}_7)(\text{OH})_3$ ), and 5.6% hausmannite ( $\text{Mn}^{2+}\text{Mn}^{3+}_2\text{O}_4$ ) according to the Diffrac Suite XRD phase analyzer software.

The ore deposit had a hydrothermal origin with hydrogenetic effects caused by a high percentage of sedimentary additives (like clay) in marine beds [62]. There is a paragenesis rich in manganese mineralization accompanying hematite. The EDS mapping analysis results, which were created from the SEM image area, revealed the elemental distribution of the sample (Fig. 5).

### 3.2 Leaching Tests Based on the Hybrid Test Design

The reactions representing the iron and manganese (IV) oxide dissolution in oxalic acid are shown in Eqs. 3 and 4. The total reaction for sulfuric acid leaching of manganiferous iron ores is shown in Eq. 5.



The test conditions and metal extraction values (Fe and Mn) based on hybrid test design are given in Table 3.

The results showed that the manganese dissolution with increasing sulfuric acid concentration was less than that of increasing oxalic acid concentration. Manganese extraction values slightly increased after 0.75 M of sulfuric acid and 30 g/L oxalic acid medium (Fig. 6a). The iron content was not as high as the manganese content in the leach solutions at each step. At room temperature and 90 min of leaching time,

**Table 1** Size-wise element analysis

Particle size ( $\mu\text{m}$ )	Contents (%)	
	Fe	Mn
0–106	27.92	14.10
106–300	30.26	14.41
300–600	32.33	14.79
600–850	32.42	14.64
850–1120	34.76	14.95
1120–3150	32.33	16.42
3150–5600	31.70	15.10
5600–7000	32.24	15.18

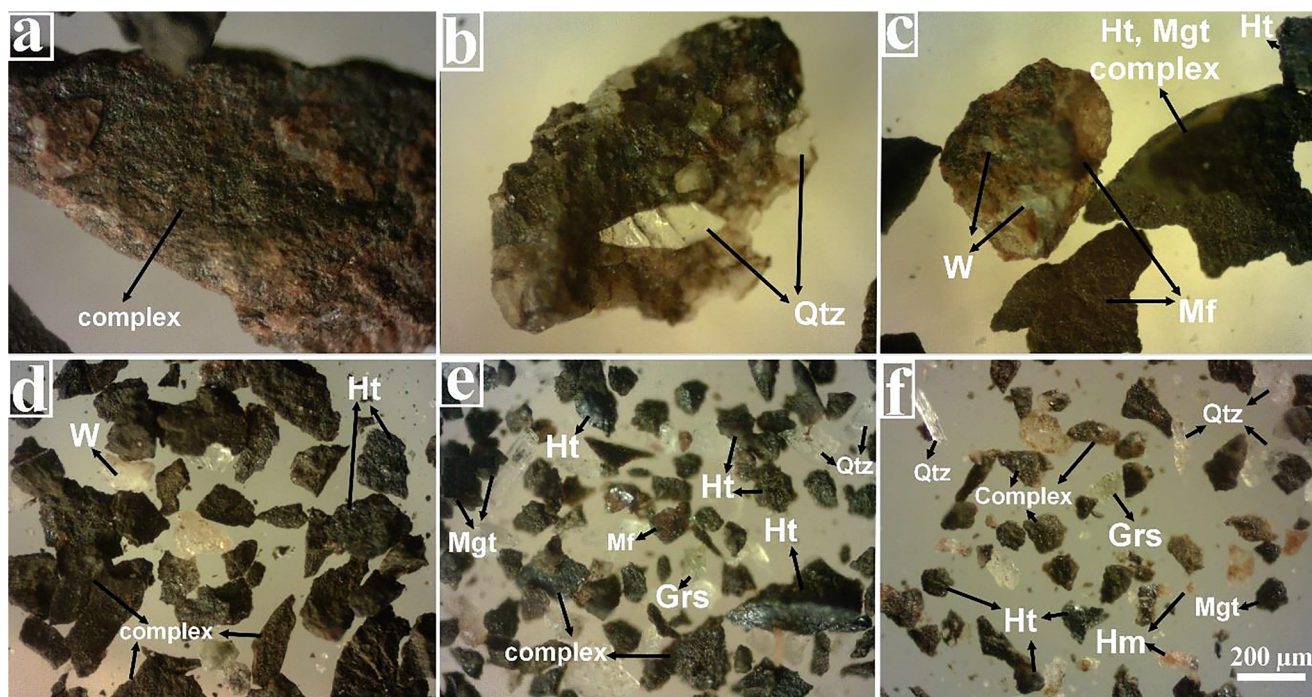


**Fig. 3** Microscope images of the ground particles (**a** + 850–1120 μm, **b** + 425–850 μm, **c** + 300–425 μm, **d** + 106–300 μm, **e** and **f** 0–106 μm; Qtz, quartz; Ht, hematite; Mgt, manganite; W, wollastonite; Mf, macfallite; Grs, grossular)

about 35% Mn dissolved and only about 4% Fe was co-dissolved. Iron dissolutions were more dependent on sulfuric acid concentration (Fig. 6b). The lower the concentration of oxalic acid, the more time needed to dissolve Mn. The Mn dissolution rate was 20% at an oxalic acid concentration of 10 g/L. Nevertheless, this rate reached 35% at a concentration of > 30 g/L (Fig. 6c). The highest manganese dissolution values were obtained by a concentration of 0.75 M of sulfuric acid after 90 min (Fig. 6d). Both iron and manganese extraction values topped out by the synergistic effects of sulfuric acid and oxalic acid.

Multiple regression analysis applied for the determination of variable interactions was based on a nonlinear model which is given in Eq. 6.

$$f(x) = M \times A^x \times B^y \times C^z \tag{6}$$

where *M* is constant, *A* and *B* denote the molar concentration of H<sub>2</sub>SO<sub>4</sub> (M) and C<sub>2</sub>H<sub>2</sub>O<sub>4</sub> (g/L), respectively, and *C* is the leaching duration (min).

Boundary conditions of the independent variables considered in multiple regression analyses were selected as 0.4–1.1 M for H<sub>2</sub>SO<sub>4</sub>, 1.72–58.28 g/L for C<sub>2</sub>H<sub>2</sub>O<sub>4</sub>, and 5–133 min for leaching time from the experimental hybrid

design conditions. Using these boundary conditions, the analytical model in Eq. 6 was solved according to the Cholesky decomposition method by the applying least squares technique. The equation parameters (*M*, *x*, *y*, and *z*) were evaluated separately for both dissolution rates (Fe and Mn). The results are given in Table 4 and the significant relationships were obtained.

The dissolution formulations are presented in Eqs. 7 and 8 as:

$$\text{Fe extraction (\%)} = 0.91 \times A^{0.77} \times B^{0.11} \times C^{0.23} \tag{7}$$

$$\text{Mn extraction (\%)} = 9.74 \times A^{0.16} \times B^{0.13} \times C^{0.17} \tag{8}$$

The estimated values of the parameters (exponentials for the formulations) indicate that sulfuric acid concentration and leaching time were the most significant parameters for Fe and Mn dissolution, respectively.

### 3.3 Effect of Temperature on Leaching

In accordance with the results of the design of experiments, the leaching experiments were performed using 0.75 M of H<sub>2</sub>SO<sub>4</sub> solution and 30 g/L C<sub>2</sub>H<sub>2</sub>O<sub>4</sub> at various temperatures ranging from 25 to 80 °C (Table 5). The stirring speed

**Table 2** Chemical analysis of the sample

Contents	SiO <sub>2</sub>	Al <sub>2</sub> O <sub>3</sub>	CaO	Fe <sub>2</sub> O <sub>3</sub>	MnO	K <sub>2</sub> O	TiO <sub>2</sub>	CuO	ZnO	PbO	LOI
%	19.02	10.13	10.02	39.91	16.30	0.11	0.32	0.17	0.05	0.17	3.80

Fig. 4 XRD pattern of the sample

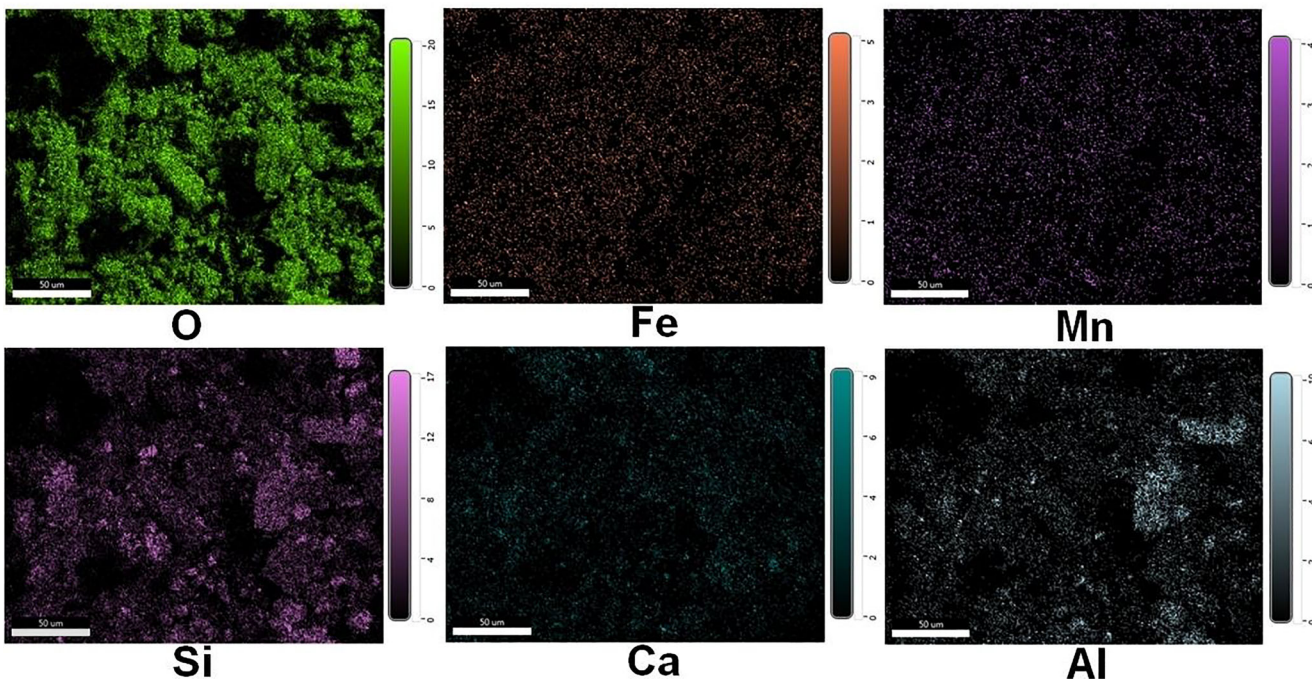
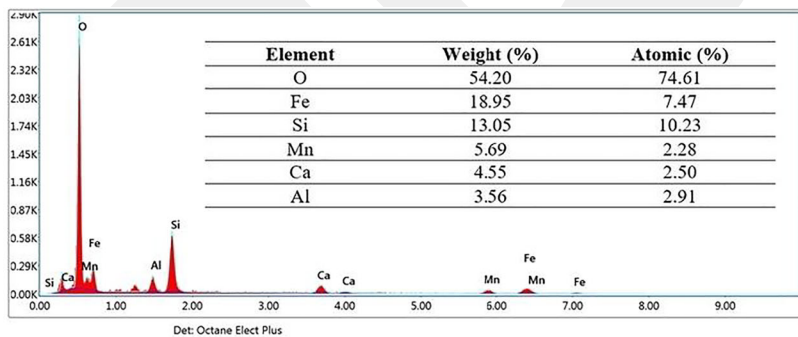
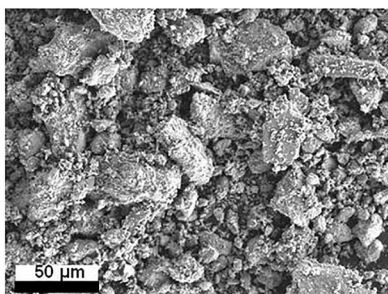
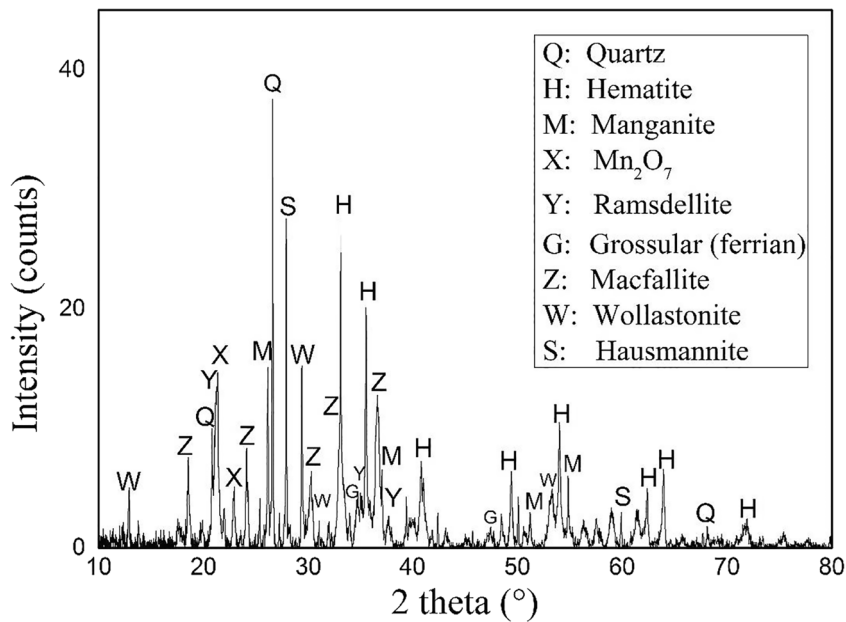


Fig. 5 EDS mapping analysis of the sample

**Table 3** Test conditions and results according to the hybrid design

Test no.	H <sub>2</sub> SO <sub>4</sub> molarity (M)	C <sub>2</sub> H <sub>2</sub> O <sub>4</sub> concentration (g/L)	Leaching time (min)	Fe (%)	Mn (%)
1	1.00	50.00	132.43	5.02	35.57
2	0.75	30.00	5.15	1.45	17.41
3	0.50	10.00	132.43	1.73	27.55
4	0.40	30.00	47.57	2.10	26.67
5	1.00	10.00	132.42	4.15	31.33
6	0.75	30.00	90.00	2.40	34.51
7	0.50	50.00	132.43	2.56	32.50
8	0.75	30.00	175.00	3.16	35.22
9	0.75	58.28	47.57	2.54	32.72
10	0.75	1.72	47.57	1.96	18.27
11	1.10	30.00	47.57	3.61	31.40

(400 rpm) and solid/liquid ratio (67 g/L) values were constant. The results showed that the increases in temperature led to increases in the speed of Mn dissolution. It was found that

after 60 min of leaching, the speed of manganese dissolution was decreased. After the first hour at 80 °C, 90.49% of Mn was dissolved. The Mn dissolutions at 75 and 90 min, however, were only increased to 91.51% and 91.93%, respectively. Although iron extraction increased with the increase in temperature, it remained at 6.78% at the end of the first hour. The rate of Fe dissolution at 80 °C was increased by 500% compared with its dissolution at 25 °C. Similar dissolution rates for both Fe and Mn were observed in the previous studies [63, 64].

The results of the XRD analysis of the residues, shown in Fig. 7, revealed that the vast majority of manganese minerals such as manganite, macfallite, and hausmannite was dissolved at > 70 °C after 90 min. Despite the decrease in the intensity of all manganese peaks in the leaching process at 25 °C, only the hausmannite peak was lost. The manganite mineral dissolution was completed at 60 °C. As a result of the extraction at 80 °C, all manganese mineral peaks except Mn<sub>2</sub>O<sub>7</sub> disappeared. XRD results confirmed that reduction of 7-valent manganese compounds was more difficult than reducing 4-valent manganese complexes. Because of the dissolution of

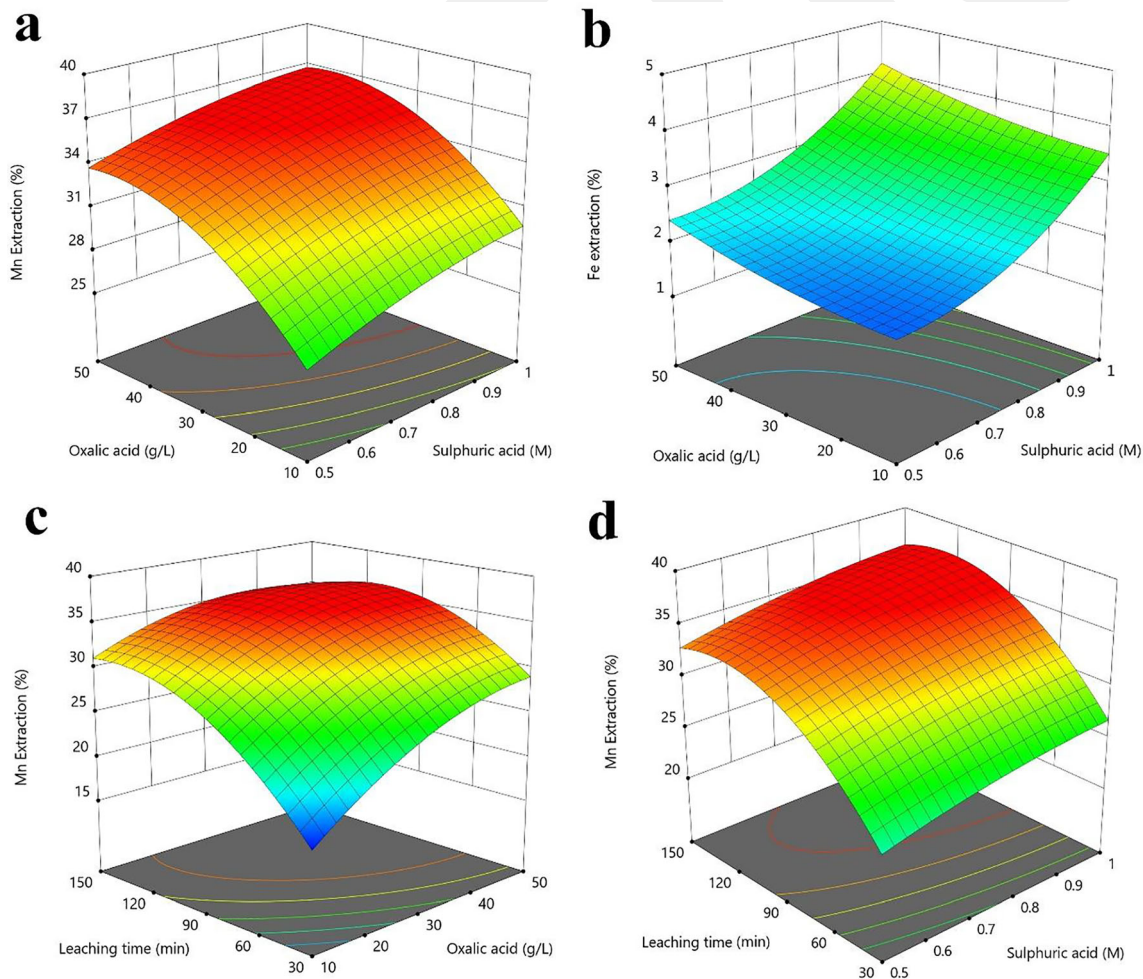


**Fig. 6** 3D graphs for hybrid design (factors that are not included are at medium values)

**Table 4** Multiple regression analysis results

Fe extraction						Mn extraction					
Independent variable	Estimate	Std. error	<i>t</i> value	<i>t</i> value tabulated (confidence level = 90%)	<i>R</i> <sup>2</sup>	Independent variable	Estimate	Std. error	<i>t</i> value	<i>t</i> value tabulated (Confidence level = 90%)	<i>R</i> <sup>2</sup>
Constant ( <i>M</i> )	0.91	0.330	2.76	1.415	0.86	Constant ( <i>M</i> )	9.74	1.420	6.85	1.415	0.93
H <sub>2</sub> SO <sub>4</sub> ( <i>A</i> )	0.77	0.180	4.28			H <sub>2</sub> SO <sub>4</sub> ( <i>A</i> )	0.16	0.065	2.46		
C <sub>2</sub> H <sub>2</sub> O <sub>4</sub> ( <i>B</i> )	0.11	0.057	1.93			C <sub>2</sub> H <sub>2</sub> O <sub>4</sub> ( <i>B</i> )	0.13	0.025	5.20		
Time ( <i>C</i> )	0.23	0.070	3.28			Time ( <i>C</i> )	0.17	0.026	6.54		

manganese minerals, quartz and hematite peaks became dominant after 90 min.

SEM images of the fed and leached (at 80 °C and 1 h) samples are shown in Fig. 8. The leaching process destroyed the rigid and angular structures characterizing the surface morphologies of manganiferous iron ores (Fig. 8a). The particle surfaces exposed to chemical abrasion indicated the effect of the leaching process. Altered lumpy structures were observed (Fig. 8b).

The dissolution kinetics of Mn was studied using extraction values (*C<sub>t</sub>*) versus time at different temperatures. The plots, represented in Fig. 9, showed that Mn dissolution reactions followed second-order kinetics. Values of 1/*C<sub>t</sub>* against temperatures (K) was a straight line with slope *k* (reaction rate coefficient). After the *k* values were determined, the Arrhenius plot was constructed in accordance with the ln(*k*) in ordinate and (1/*T*) in abscissa. The Arrhenius plot was given in Supplementary file 1 (Fig. S1). The square of the correlation (*R*<sup>2</sup>) was 98%. According to the Arrhenius plot, which slope gave  $-E_a/R$  equation of the reaction, the activation energy (*E<sub>a</sub>*) was calculated to be 53.38 kJ/mol. The *E<sub>a</sub>* value is in good agreement with those found in the previous studies [65–67].

The *E<sub>a</sub>* values of diffusion-controlled reactions are commonly less than 21 kJ/mol, while the ones in the processes that the chemical reaction is the rate-determining stage vary between 40 and 100 kJ/mol. In addition, chemically controlled reactions are intensely dependent on temperature [68, 69].

Accordingly, it was determined that the Mn dissolution reactions in this study were chemically controlled.

### 3.4 Magnetic Separation

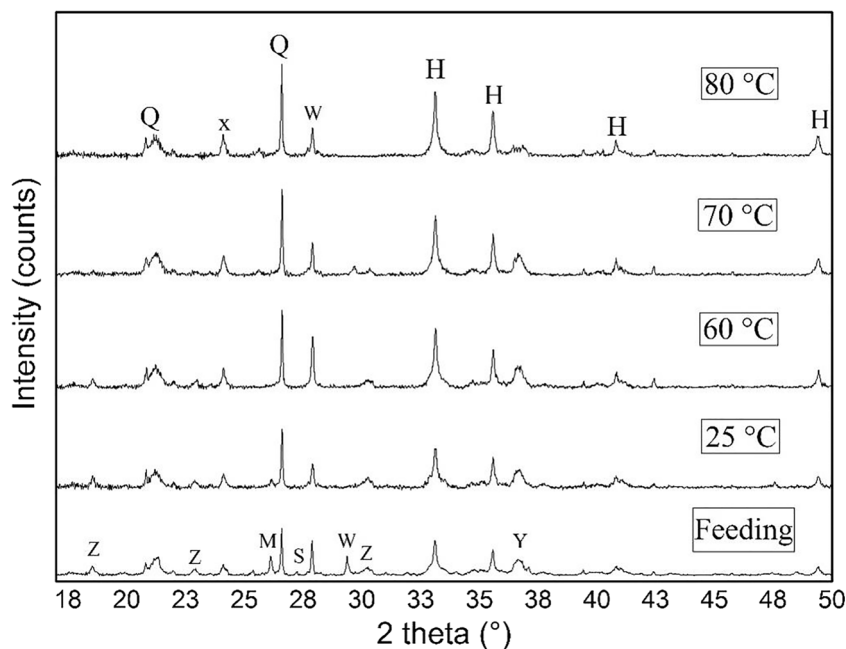
Hematite mineral and most of the manganese minerals are paramagnetic [70, 71]. Magnetizations of the leach residue (obtained at 80 °C and 1 h leach duration), original feed sample, and iron-rich magnetic product after separation (obtained at 1 T magnetic field intensity) were determined using the Physical Property Measurement System (PPMS) equipped with the vibrating-sample magnetometer (VSM) head at ambient temperature (Fig. 10). After the first hour of the leaching process wherein the majority of manganese was dissolved, the concentration of iron in the leached residue was increased. The dissolution of the calcium and aluminum also contributed to the increase in iron concentration. The increased convexity observed in leach residue represents growth in magnetization due to the higher magnetic material amount compared with the original feed sample. It was found that the ferromagnetic behavior in the M-H plots increased after leaching.

Magnetic separation tests were carried out to the unleached samples and the leached residues, separately. The residues obtained under the following conditions were used in magnetic separation tests: 0.75 M H<sub>2</sub>SO<sub>4</sub>, 30 g/L C<sub>2</sub>H<sub>2</sub>O, 400 rpm stirring speed, 80 °C temperature, 67 g/L solid/liquid ratio, and 1 h leaching time. These leaching residues, which

**Table 5** Dissolution of Fe and Mn at different temperatures

Time (min)	25 °C		60 °C		70 °C		80 °C	
	Fe (%)	Mn (%)	Fe (%)	Mn (%)	Fe (%)	Mn (%)	Fe (%)	Mn (%)
15	0.36	13.55	0.92	44.88	1.37	53.39	2.01	66.79
30	0.65	17.77	1.11	49.77	2.06	59.80	3.72	78.46
45	0.95	19.88	1.50	54.97	2.99	66.88	5.41	86.19
60	1.24	22.77	2.07	60.77	4.00	72.79	6.78	90.49
75	1.90	27.50	3.15	66.88	4.89	78.44	8.59	91.51
90	2.40	31.25	4.03	73.77	6.72	80.00	10.88	91.93

**Fig. 7** XRD analyses of the residues after 90 min (Q, quartz; H, hematite; M, Manganite; X, Mn<sub>2</sub>O<sub>7</sub>; Y, ramsdellite; Z, macfallite; W, wollastonite; S, hausmannite)



contained 42.03% Fe and 1.14% Mn, were selected since the high Mn dissolution and the low Fe loss were achieved at this condition. In both separations, Mn and Fe yields increased with increasing magnetic field strength but the product grades decreased. Correspondingly, in the tests with low magnetic field strength, the yields were very low but the grades were high. As the magnetic field intensities increased, the yields increased in accordance with specific properties of the paramagnetic materials. The increase in the magnetic moment value of the magnetic product recovered from the leached residue after magnetic separation at 1 T magnetic field strength shown in Fig. 10. The magnetic moment of the product is about 2 times higher than the leached residue, which was not dissolved under the optimum reductive leaching condition. The M-H diagram demonstrates that the insoluble and

ferromagnetic iron content can be recovered as a magnetic product. The yields of the magnetic separation from the leached residues were higher than from unleached samples (Table 6). As a result of the dissolution of Fe- and Mn-bearing particles, some of the particles that had magnetic properties altered into non-magnetic particles resulted in higher yields of the magnetic separation. In particular, the dissolution of Mn, which was over 90%, led to indirect mineral liberation and caused higher yields. The Fe grades of the recovered magnetic product were higher than 56%. Moreover, Mn grades of these concentrates were below 2.35% allowing the magnetic product to be classified as salable iron ore products. Magnetic separation test results found in the literature support the findings of this study [72–74].

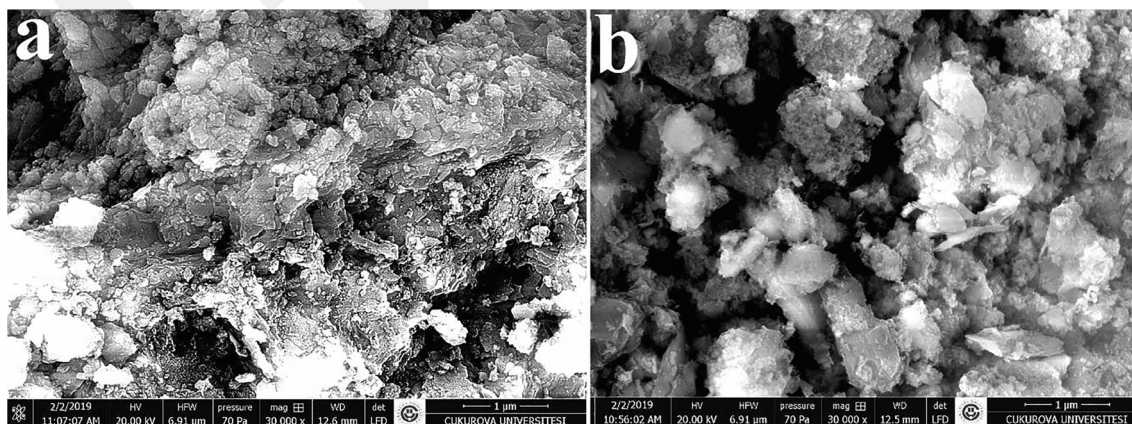
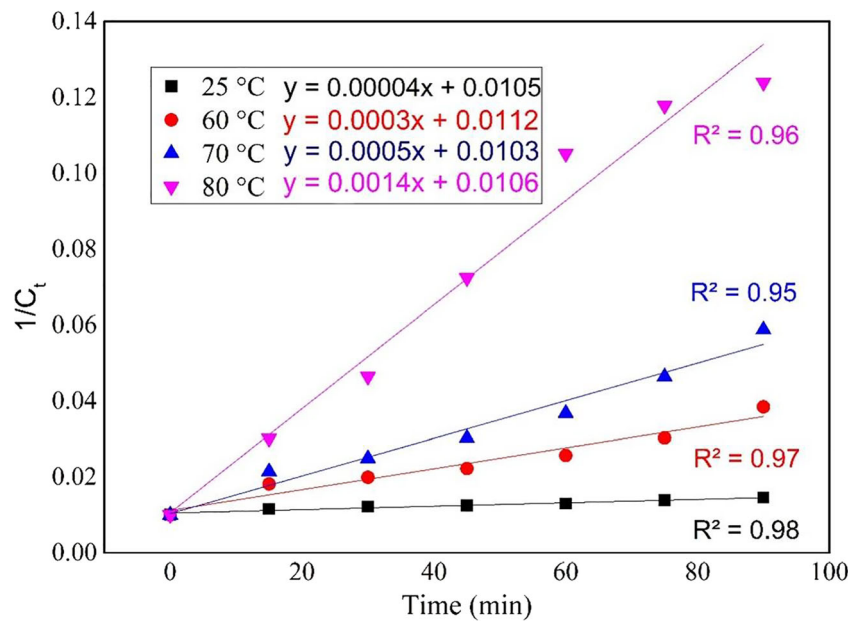


**Fig. 8** Micrographs of the untreated (a) and treated (b) samples

**Fig. 9** Second-order kinetics of Mn dissolution



## 4 Conclusions

The present study demonstrated that more than 90% of manganese can be selectively dissolved from manganiferous iron ores by reductive leaching using  $\text{H}_2\text{SO}_4$  as lixiviant and  $\text{C}_2\text{H}_2\text{O}_4$  as reductant. The results of the hybrid test design performed at ambient temperature showed that the concentration of reductant was more influential to the leaching process in terms of Mn dissolution, whereas sulfuric acid concentration was more influential for Fe dissolution. Mn dissolution

reactions were found to be chemically controlled reactions since its dissolution was highly dependent on temperature and the activation energy was higher than 40 kJ/mol. The optimal selective leaching conditions, under which 90.49% Mn and 6.78% Fe were dissolved, were found to be  $\text{H}_2\text{SO}_4$  concentration 0.75 M,  $\text{C}_2\text{H}_2\text{O}_4$  concentration 30 g/L, leaching temperature 80 °C, solid/liquid ratio 67 g/L, leaching time 60 min, stirring speed 400 rpm, and particle size 0–106  $\mu\text{m}$ . The magnetic product obtained in the present study contained > 56% Fe and low amounts of Mn impurities (< 5%) that suit

**Fig. 10** M-H curves of the materials

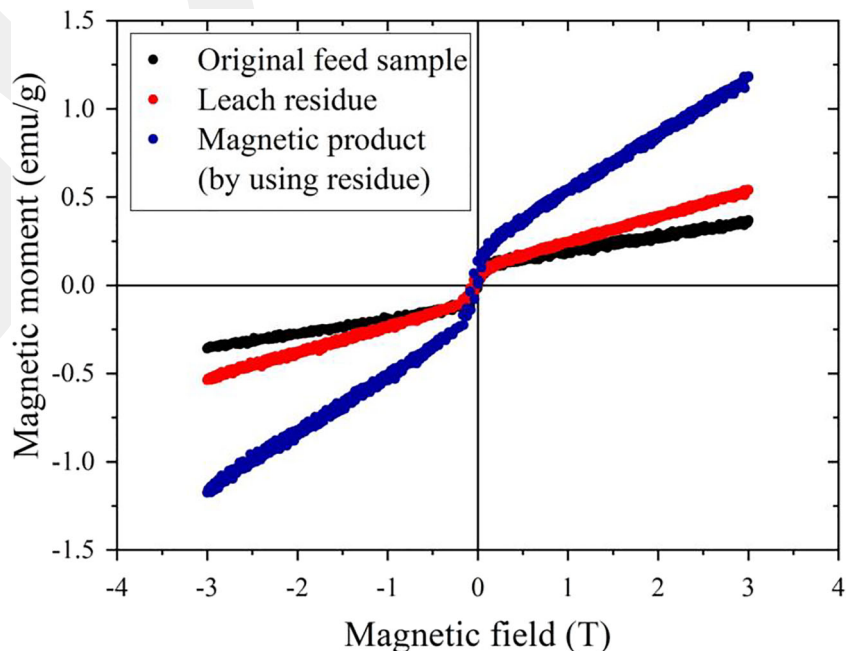


**Table 6** Magnetic separation test results before and after leaching

Magnetic field strength (T)	Before the leaching				After the leaching			
	Grades (%)		Recovery yields (%)		Grades (%)		Recovery yields (%)	
	Fe	Mn	Fe	Mn	Fe	Mn	Fe	Mn
0.25	42.88	18.55	12.29	11.76	59.11	2.35	17.73	25.77
0.50	36.45	17.14	17.95	18.67	58.34	2.22	31.23	43.82
0.75	33.38	16.14	28.70	30.68	57.78	2.09	42.62	56.83
1.00	31.59	14.48	43.74	44.34	56.69	1.97	51.35	61.67
1.25	31.14	14.64	48.80	50.73	56.20	1.79	56.83	66.73
1.50	31.56	13.80	54.55	52.75	54.60	1.65	62.62	68.03
1.75	31.01	13.63	58.05	56.42	54.32	1.50	66.83	67.13

sintered ore qualities in line with the demands of the iron and steel industry. This product was obtained from the leached residues collected from the optimum leach conditions by high-intensity wet magnetic separation. The magnetic separation tests were also applied directly to the unleached sample at a size fraction of – 106- $\mu$ m size. In these tests, the Fe grades were between 30 and 43%. It is planned to apply hematite-magnetite conversion by a microwave-assisted carbothermal reduction method to increase the iron recovery yields in magnetic separation for further studies.

## Compliance with Ethical Standards

**Conflict of Interest** The author declares that there is no conflict of interest.

## References

- Ding J, Chai T, Cheng W, Zheng X (2015) Data-based multiple-model prediction of the production rate for hematite ore beneficiation process. *Control Eng Pract* 45:219–229. <https://doi.org/10.1016/j.conengprac.2015.08.015>
- He J, Liu C, Xie J, Hong P, Yao Y (2017) Beneficiation of coarse particulate iron ore by using a dry density-based fluidized bed separator. *Powder Technol* 319:346–355. <https://doi.org/10.1016/j.powtec.2017.07.007>
- Shrimali K, Yin X, Wang X, Miller JD (2017) Fundamental issues on the influence of starch in amine adsorption by quartz. *Colloids Surf A Physicochem Eng Asp* 522:642–651. <https://doi.org/10.1016/j.colsurfa.2017.03.031>
- Kuleshov V, Maynard JB (2017) Isotope geochemistry: the origin and formation of manganese rocks and ores. Elsevier, Amsterdam
- Nurjaman F, Amarela S, Noegroho A, Ferdian D, Suharno B (2017) Beneficiation of two different low-grade Indonesian manganese ores to improve the Mn/Fe ratio. In: AIP Conference Proceedings 1823:020021:1–7. <https://doi.org/10.1063/1.4978094>
- USGS 2008 and 2018, Manganese statistics and information. <https://minerals.usgs.gov/minerals/pubs/commodity/manganese/>. Accessed time: 25.01.2019
- USGS, 2008 and 2018, Iron ore statistics and information. <https://www.usgs.gov/centers/nmic/iron-ore-statistics-and-information>. Accessed time: 25.01.2019
- Gutzmer J, Beukes NJ (2009) Iron and manganese ore deposits: mineralogy, geochemistry, and economic geology. In: De Vivo B, Grasemann B, Stüwe K (eds) *Geology*, vol IV. EOLSS publishers, France, pp 43–69
- IBOM (Indian Bureau of Mines) (2014) Manganese ore – vision 2020 and beyond. [https://ibm.gov.in/writereaddata/files/11052014103838Manganese\\_Ore\\_Vision\\_2020\\_and\\_Beyond.pdf](https://ibm.gov.in/writereaddata/files/11052014103838Manganese_Ore_Vision_2020_and_Beyond.pdf). Accessed 11 Oct 2018
- Mukherjee A, Raichur AM, Natarajan KA, Modak JM (2004) Recent developments in processing ocean manganese nodules—a critical review. *Miner Process Extr Metall Rev* 25(2):91–127. <https://doi.org/10.1080/08827500490433188>
- Biswas A, Chakraborti N, Sen PK (2009) A genetic algorithms based multi-objective optimization approach applied to a hydrometallurgical circuit for ocean nodules. *Miner Process Extr Metall Rev* 30(2):163–189. <https://doi.org/10.1080/08827500802397284>
- Jana RK, Pandey BD, Premchand (1999) Ammoniacal leaching of roast reduced deep-sea manganese nodules. *Hydrometallurgy* 53: 45–56. [https://doi.org/10.1016/S0304-386X\(99\)00031-6](https://doi.org/10.1016/S0304-386X(99)00031-6)
- Randhawa NS, Jana RK, Das NN (2013) Silicomanganese production utilising low grade manganese nodules leaching residue. *Miner Process Ext Metall* 122(1):6–14. <https://doi.org/10.1179/1743285512Y.0000000022>
- Vapur H, Top S, Altiner M, Uçkun Ş, Sarıkaya M (2019) Comparison of iron ores upgraded with Falcon concentrator and magnetic separators assisted by coal reduction-conversion process. *Part Sci Technol* 1–10. <https://doi.org/10.1080/02726351.2018.1548532>
- Shrimali K, Atluri V, Wang Y, Bacchuwar S, Wang X, Miller JD (2018) The nature of hematite depression with corn starch in the reverse flotation of iron ore. *J Colloid Interface Sci* 524:337–349. <https://doi.org/10.1016/j.jcis.2018.04.002>
- Yu J, Han Y, Li Y, Gao P (2017) Beneficiation of an iron ore fines by magnetization roasting and magnetic separation. *Int J Miner Process* 168:102–108. <https://doi.org/10.1016/j.minpro.2017.09.012>
- Mehdilo A, Irannajad M, Hojjati-Rad MR (2013) Characterization and beneficiation of Iranian low-grade manganese ore. *Physicochem Probl Miner Process* 49:725–741. <https://doi.org/10.5277/ppmp130230>
- Mishra PP, Mohapatra BK, Mahanta K (2009) Upgradation of low-grade siliceous manganese ore from Bonaï-Keonjhar Belt, Orissa, India. *J Miner Mater Charact Eng* 8:47–56. <https://doi.org/10.4236/jmmce.2009.81005>
- Tripathy SK, Banerjee PK, Suresh N (2015) Effect of desliming on the magnetic separation of low-grade ferruginous manganese ore. *Int J Miner Mater* 22:661–673. <https://doi.org/10.1007/s12613-015-1120-0>
- Bayat O, Altiner M, Top S (2013) Investigation of the beneficiation of low grade manganese ores. In: 23<sup>rd</sup> International Mining Congress and Exhibition of Turkey, IMCET, 951–958
- Yapici N, Altiner M (2013) Investigation of geological and ore enrichment of the manganese deposit in Tomarza/Seyhbarak (Kayseri) region. *Çukurova University Journal of the Faculty of Engineering and Architecture. TÜBİTAK (The Scientific and Technological Research Council of Turkey)* 28:1–9
- Singh V, Ghosh TK, Ramamurthy Y, Tathavadkar V (2011) Beneficiation and agglomeration process to utilize low-grade ferruginous manganese ore fines. *Int J Miner Process* 99:84–86. <https://doi.org/10.1016/j.minpro.2011.03.003>
- Singh V, Biswas A (2017) Physicochemical processing of low grade ferruginous manganese ores. *Int J Miner Process* 158:35–44. <https://doi.org/10.1016/j.minpro.2016.11.013>

24. Naik PK, Sukla LB, Das SC (2002) Application of statistical design in the leaching study of low-grade manganese ore using aqueous sulfur dioxide. *Sep Sci Technol* 37(6):1375–1389. <https://doi.org/10.1081/SS-120002616>
25. Nayl AA, Ismail IM, Aly HF (2011) Recovery of pure  $MnSO_4 \cdot H_2O$  by reductive leaching of manganese from pyrolusite ore by sulfuric acid and hydrogen peroxide. *Int J Miner Process* 100(3–4):116–123. <https://doi.org/10.1016/j.minpro.2011.05.003>
26. Zhang Y, Du M, Liu B, Su Z, Li G, Jiang T (2017) Separation and recovery of iron and manganese from high-iron manganese oxide ores by reduction roasting and magnetic separation technique. *Sep Sci Technol* 52(7):1321–1332. <https://doi.org/10.1080/01496395.2017.1284864>
27. Hsiaohong C, Chongyue F (1995) Leaching of manganese nodule in dilute acid solutions in presence of zinc sulfide concentrate. *Miner Process Extr Metall Rev* 15(1–4):95–100. <https://doi.org/10.1080/08827509508914188>
28. Naik PK, Natharma KC, Das SC, Misra VN (2003) Leaching of low grade Joda manganese ore with sulphur dioxide in aqueous medium. *Miner Process Ext Metall* 112(2):131–134. <https://doi.org/10.1179/037195503225002817>
29. Gao H, Jiang T, Xu Y, Wen J, Xue X (2018) Leaching kinetics of vanadium and chromium during sulfuric acid leaching with microwave and conventional calcification-roasted high chromium vanadium slag. *Miner Process Extr Metall Rev* 1–10. <https://doi.org/10.1080/08827508.2018.1538985>
30. Gao Y, Olivas-Martinez M, Sohn HY, Kim HG, Kim CW (2012) Upgrading of low-grade manganese ore by selective reduction of iron oxide and magnetic separation. *Metall Mater Trans B Process Metall Mater Process Sci* 43:1465–1475. <https://doi.org/10.1007/s11663-012-9731-6>
31. Gao L, Liu Z, Chu M, Wang R, Wang Z, Feng C (2018) Upgrading of low-grade manganese ore based on reduction roasting and magnetic separation technique. *Sep Sci Technol* 54:195–206. <https://doi.org/10.1080/01496395.2018.1504795>
32. Liu B, Zhang Y, Wang J, Wang J, Su Z, Li G, Jiang T (2019) A further investigation on the  $MnO_2$ - $Fe_2O_3$  system roasted under  $CO$ - $CO_2$  atmosphere. *Adv Powder Technol* 30:302–310. <https://doi.org/10.1016/j.apt.2018.11.006>
33. Liu B, Zhang Y, Wang J, Wang J, Su J, Li G, Jiang T (2018) New understanding on separation of Mn and Fe from ferruginous manganese ores by the magnetic reduction roasting process. *Appl Surf Sci* 444:133–144. <https://doi.org/10.1016/j.apsusc.2018.02.234>
34. Sahoo RN, Naik PK, Das SC (2001) Leaching of manganese from low-grade manganese ore using oxalic acid as reductant in sulphuric acid solution. *Hydrometallurgy* 62:157–163. [https://doi.org/10.1016/S0304-386X\(01\)00196-7](https://doi.org/10.1016/S0304-386X(01)00196-7)
35. Hariprasad D, Dash B, Ghosh MK, Anand S (2017) Leaching of manganese ores using sawdust as a reductant. *Miner Eng* 20:1293–1295. <https://doi.org/10.1016/j.mineng.2007.07.013>
36. Zhuo C, Zhu G, Zhao Y (2009) Study in reduction-roast leaching manganese from low-grade manganese dioxide ores using cornstalk as reductant. *Hydrometallurgy* 96:176–179. <https://doi.org/10.1016/j.hydromet.2008.08.004>
37. Lasheen TA, El Hazek MN, Helal AS, El-Nagar W (2009) Recovery of manganese using molasses as reductant in nitric acid solution. *Int J Miner Process* 92:109–114. <https://doi.org/10.1016/j.minpro.2009.03.001>
38. Furlani G, Moscardini E, Pagnanelli F, Ferella F, Vegliò F, Toro L (2009) Recovery of manganese from zinc alkaline batteries by reductive acid leaching using carbohydrates as reductant. *Hydrometallurgy* 99:115–118. <https://doi.org/10.1016/j.hydromet.2009.07.005>
39. Ismail AA, Ali EA, Ibrahim A, Ahmed MSA (2004) Comparative study on acid leaching of low grade manganese ore using some industrial wastes as reductants. *Can J Chem Eng* 82:1296–1300. <https://doi.org/10.1002/cjce.5450820618>
40. Tian X, Wen X, Yang C, Liang Y, Pi Z, Wang Y (2010) Reductive leaching of manganese from low-grade manganese oxide ores using corncob as reductant in sulfuric acid solution. *Hydrometallurgy* 100:157–160. <https://doi.org/10.1016/j.hydromet.2009.11.008>
41. Kurşunoğlu S, Kaya M (2013) Recovery of manganese from spent batteries using guar meal as a reducing agent in a sulfuric acid medium. *Ind Eng Chem Res* 52:18076–18084. <https://doi.org/10.1021/ie401682f>
42. Tang Q, Zhong H, Wang S, Li J, Liu G (2014) Reductive leaching of manganese oxide ores using waste tea as reductant in sulfuric acid solution. *Trans Nonferrous Metals Soc* 24:861–867. [https://doi.org/10.1016/S1003-6326\(14\)63136-8](https://doi.org/10.1016/S1003-6326(14)63136-8)
43. Li C, Zhong H, Wang S, Xue J, Wu F, Zhang Z (2015) Manganese extraction by reduction–acid leaching from low-grade manganese oxide ores using CaS as reductant. *Trans Nonferrous Metals Soc* 25:1677–1684. [https://doi.org/10.1016/S1003-6326\(15\)63772-4](https://doi.org/10.1016/S1003-6326(15)63772-4)
44. Xiong S, Li X, Liu P, Hao S, Hao F, Yin Z, Liu J (2018) Recovery of manganese from low-grade pyrolusite ore by reductively acid leaching process using lignin as a low cost reductant. *Miner Eng* 125:126–132. <https://doi.org/10.1016/j.mineng.2018.06.003>
45. Sun Y, Fu G, Jiang L (2018) Reductive leaching of low-grade manganese oxide ores using pretreated straw as reductant. *Miner Process Ext Metall* 1–6. <https://doi.org/10.1080/25726641.2018.1505210>
46. Fuerstenau DW, Han KN (1983) Metallurgy and processing of marine manganese nodules. *Miner Process Extr Metall Rev* 1(1–2):1–83. <https://doi.org/10.1080/08827508308952589>
47. Sobianowska-Turek A, Szczepaniak W, Maciejewski P, Gawlik-Kobylińska M (2016) Recovery of zinc and manganese, and other metals (Fe, Cu, Ni, Co, Cd, Cr, Na, K) from Zn- $MnO_2$  and Zn-C waste batteries: hydroxyl and carbonate co-precipitation from solution after reducing acidic leaching with use of oxalic acid. *J Power Sources* 325:220–228. <https://doi.org/10.1016/j.jpowsour.2016.06.042>
48. Sinha MK, Purcell W (2019) Reducing agents in the leaching of manganese ores: a comprehensive review. *Hydrometallurgy* 187:168–186. <https://doi.org/10.1016/j.hydromet.2019.05.021>
49. Liu B, Zhang Y, Lu M, Su Z, Li G, Jiang T (2019) Extraction and separation of manganese and iron from ferruginous manganese ores: a review. *Miner Eng* 131:286–303. <https://doi.org/10.1016/j.mineng.2018.11.016>
50. Azizi D, Shafaei SZ, Noaparast M, Abdollahi H (2012) Modeling and optimization of low-grade Mn bearing ore leaching using response surface methodology and central composite rotatable design. *Trans Nonferrous Metals Soc* 22(9):2295–2305. [https://doi.org/10.1016/S1003-6326\(11\)61463-5](https://doi.org/10.1016/S1003-6326(11)61463-5)
51. Sayilgan E, Kukrer T, Ferella F, Akcil A, Veglio F, Kitis M (2009) Reductive leaching of manganese and zinc from spent alkaline and zinc–carbon batteries in acidic media. *Hydrometallurgy* 97:73–79. <https://doi.org/10.1016/j.hydromet.2009.01.004>
52. El Hazek MN, Gabr A (2016) Dissolution of manganese from polycrystalline material using sulfuric-oxalic acid medium. *Am J Anal Chem* 7:469–477. <https://doi.org/10.4236/ajac.2016.75044>
53. Astuti W, Mufakhir FR, Prasetyo E, Sumardi S, Yuda APT, Nurjaman F, Supriyatna YI, Handoko AS (2019) Reductive-atmospheric leaching of manganese from pyrolusite ore using various reducing agents. In: *AIP Conference Proceedings* 2097:030117:1–6. <https://doi.org/10.1063/1.5098292>
54. Pagnanelli F, Furlani G, Valentini P, Vegliò F, Toro L (2004) Leaching of low-grade manganese ores by using nitric acid and glucose: optimization of the operating conditions. *Hydrometallurgy* 75(1–4):157–167. <https://doi.org/10.1016/j.hydromet.2004.07.007>

55. El Hazek MN, Lasheen TA, Helal AS (2006) Reductive leaching of manganese from low grade Sinai ore in HCl using H<sub>2</sub>O<sub>2</sub> as reductant. *Hydrometallurgy* 84(3–4):187–191. <https://doi.org/10.1016/j.hydromet.2006.05.006>
56. Vapur H, Top S (2016) Improving of quality properties of the specularite ore. *Çukurova University Journal of the Faculty of Engineering and Architecture. TÜBİTAK (The Scientific and Technological Research Council of Turkey)* 31:293–300
57. Baioumy HM, Khedr MZ, Ahmed AH (2013) Mineralogy, geochemistry and origin of Mn in the high-Mn iron ores, Bahariya Oasis, Egypt. *Ore Geol Rev* 53:63–76. <https://doi.org/10.1016/j.oregeorev.2012.12.009>
58. Rath SS, Tripathy SK, Rao DS, Biswal SK (2018) Characterization and reduction roasting studies of an iron rich manganese ore. *T Indian I Metals* 71:861–872. <https://doi.org/10.1007/s12666-017-1218-3>
59. MTA (2019) Mineral resources of Adana province. [http://www.mta.gov.tr/v3.0/sayfalar/bilgimerkezi/maden\\_potansiyel\\_2010/Adana\\_Madenler.pdf](http://www.mta.gov.tr/v3.0/sayfalar/bilgimerkezi/maden_potansiyel_2010/Adana_Madenler.pdf). Accessed 07 Jan 2019
60. Roquemore KG (1976) Hybrid designs for quadratic response surfaces. *Technometrics* 18:419–423. <https://doi.org/10.2307/1268657>
61. Del Castillo E (2007) Process optimization a statistical approach. Springer, USA, pp 129–130. <https://doi.org/10.1007/978-0-387-71435-6>
62. Öztürk H (1997) Manganese deposits in Turkey: distribution, types and tectonic setting. *Ore Geol Rev* 12:187–203. [https://doi.org/10.1016/S0169-1368\(97\)00005-X](https://doi.org/10.1016/S0169-1368(97)00005-X)
63. Ali S, Iqbal Y, Farooq U, Ahmad S (2016) Leaching of manganese ores using corn cob as reductant in H<sub>2</sub>SO<sub>4</sub> solution. *Physicochem Probl Miner Process* 52:56–65. <https://doi.org/10.5277/ppmp160105>
64. Feng L, Zhang S, Li H Reductive leaching of manganese from low-grade pyrolusite ore in sulfuric acid using pyrolysis-pretreated sawdust as a reductant. *Int J Miner Metall Mater* 23:241–246. <https://doi.org/10.1007/s12613-016-1232-1>
65. Sun Y, Fu G, Jiang L (2017) Kinetic study of the leaching of low-grade manganese ores by using pretreated sawdust as reductant. *Minerals* 7:1–9. <https://doi.org/10.3390/min7050083>
66. Wang Y, Jin S, Lv Y, Zhang Y, Su H (2017) Hydrometallurgical process and kinetics of leaching manganese from semi-oxidized manganese ores with sucrose. *Minerals* 7:1–13. <https://doi.org/10.3390/min7020027>
67. Hsiao hong C, Chongyue F (1995) Kinetics of leaching manganese nodules in the presence of zinc sulfide. *Miner Process Extr Metall Rev* 15(1–4):101–114. <https://doi.org/10.1080/08827509508914189>
68. Ashraf M, Zafar ZI, Ansari TM (2005) Selective leaching kinetics and upgrading of low-grade calcareous phosphate rock in succinic acid. *Hydrometallurgy* 80:286–292. <https://doi.org/10.1016/j.hydromet.2005.09.001>
69. Alaoui A, EL Kacemi K, EL Ass K, Darmane Y, Kitane S (2016) Kinetic study of the leaching of manganese mine tailings by organic reductant in sulphuric acid solution. *Miner Process Ext Metall* 125: 109–116. <https://doi.org/10.1080/03719553.2016.1164937>
70. Kropacek V, Krs M, Bucha V (1975) Magnetic properties of natural Mn-oxides. *Stud Geophys Geod* 19:261–274. <https://doi.org/10.1007/BF01614255>
71. Tripathy SK, Singh V, Murthy YR, Banerjee PK, Suresh N (2017) Influence of process parameters of dry high intensity magnetic separators on separation of hematite. *Int J Miner Process* 160:16–31. <https://doi.org/10.1016/j.minpro.2017.01.007>
72. Zhang X, Tan X, Yi Y, Liu W, Li C (2017) Recovery of manganese ore tailings by high-gradient magnetic separation and hydrometallurgical method. *JOM* 69:2352–2357. <https://doi.org/10.1007/s11837-017-2521-5>
73. Li W, Zhou L, Han Y, Zhu Y, Li Y (2019) Effect of carboxymethyl starch on fine-grained hematite recovery by high-intensity magnetic separation: experimental investigation and theoretical analysis. *Powder Technol* 343:270–278. <https://doi.org/10.1016/j.powtec.2018.11.024>
74. Dash N, Rath SS, Angadi SI (2019) Thermally assisted magnetic separation and characterization studies of a low-grade hematite ore. *Powder Technol* 346:70–77. <https://doi.org/10.1016/j.powtec.2019.02.008>

**Publisher's Note** Springer Nature remains neutral with regard to jurisdictional claims in published maps and institutional affiliations.